International Research Journal of Engineering and Technology (IRJET) e-ISSN: 2395-0056
Volume: 09 Issue: 07 | July 2022 www.irjet.net p-ISSN: 2395-0072

Simulation studies on developed Solar PV Array based Multipurpose EV Charger by using SMC Control and ANFIS

[1]P SHAMEEM [2]L SURESH

PG STUDENT (184M1D5405), DEPT.OF EEE,VEMU INSTITUTE OF TECHNOLOGY,P.KOTHAKOTA-517112
ASSISTANT PROFESSOR, DEPT.OF EEE, VEMU INSTITUTE OF TECHNOLOGY, P.KOTHAKOTA-517112

***Abstract*— In this paper, an implementation of solar photovoltaic (PV) array powered grid connected, residential electric vehicle (EV) charger is presented, which caters the need of an EV, household loads and the grid. The charger is enabled to operate autonomously using a PV array for providing an uninterruptible charging and power to household loads. However, in the absence of the PV array or insufficient PV array generation, the grid connected mode of operation is presented. Moreover, the charger is supported with the synchronization and seamless mode switching control, so that the charger automatically connects/disconnects from the grid without disturbing the EV charging and household supply. The charger is also enabled with the vehicle-to-grid (V2G) active/reactive power support to the grid and vehicle-to-home (V2H) power transfer for supporting the local loads in an islanded condition. The charger is also controlled to operate as an active power filter for achieving the unity power factor (UPF) operation and total harmonic distortion (THD) of the grid current within 5%. Moreover, for achieving energy management, a dc-link voltage regulation based energy management strategy is used and a sliding mode control (SMC) is used for regulating the dc-link voltage. For satisfactory operation under distorted voltage condition, a second-order generalized integrator frequency locked loop with dc offset rejection (SOGI-FLL-DR), is used to generate the sinusoidal reference grid current. The charger is designed for a single-phase 230V, 50Hz grid and it is experimentally validated in the laboratory.**

***Keywords*— Electric vehicle, bi-directional charger, solar PV generation, reactive power, power quality.**

I. INTRODUCTION

In the current scenario, the electric vehicle (EV) is emerging as a promising solution to the problems caused by fossil fuel- powered vehicles [1]. However, the adaptability of EV depends on the charging infrastructure [2]. The charging of EV requires a huge amount of electrical energy, which mostly comes from coal/ gas-based power plants. Therefore, in a true sense, the EVs can be a green and clean alternative to the present transport system when the electrical energy required for the charging of EV, comes from the renewable energy sources such as solar, wind etc. [3]. The advantage of this kind of charging station is that the PV array power is generated and used locally. Because of this, the transmission lines need not be upgraded for the high power. Moreover, the charging station does not require to draw power from the grid when the cost of energy is high. Another advantage of PV array-based charging station is that it is not location-specific. Ma et al. [4] have proposed the use of office building and parking area for laying down the solar PV panels, as these solar PV panels also work as a shed and prevent the heating of the vehicles and buildings. Therefore, the use of PV array-based charging station not only avoids overloading of the grid, but it also minimizes the operational cost of the charging station. Moreover, the coordinated operation of the PV array and EV mitigates the impacts of PV generation on the utility, and it eliminates the problems caused by the solar PV generation intermittency [5].

Therefore, many researchers have contributed their work for developing the PV array-based charging station. Gunter et al.
[6] and Satpathy et al. [7] have proposed the PV array and wind energy-based grid connected system. Marra et al. [8], Saxena et al. [9], Monteiro et al. [10], Tran et al. [11], and Tazay et al.
[12] have reported the implementation of the PV array-based EV charging station. However, in the literature, a dc-dc converter (mostly boost converter) is used to connect the PV array to the dc link. In this paper, the solar PV array is directly connected to the dc link. The major advantages of this topology, include the reduction in one power stage through the elimination of dc-dc converter stage, circuit complexity and the cost of the converter, without compromising the performance of the PV array. Moreover, this topology is a kind of retrofit solution wherein the PV array can be augmented to the existing charging infrastructure with minimum change in the software (maximum power point tracking control algorithm) alone.

However, if the charger is used only for charging the EV, the charger remains idle for at least 50% of the lifetime. Therefore, the converter of the charger has to be used for other tasks to improve the operational efficiency of the charger when the EV is not connected for charging. There are many functionalities proposed in the literature such as the four-quadrant operation of charger, vehicle-to-home operation using the EV battery and active filtering etc. [13]. However, in the available literature, different converters and controls are used for different modes of operation. Moreover, the charger operation is restricted by the grid availability (islanded or grid connected operation), types of mode switching among different operating modes (seamless or discontinuous) and these conditions affect the

operational efficiency of the charger. Many efforts are being made to develop an integrated system with the capability to perform the above functionalities, which are beneficial to the grid, household loads and the EVs [14]. Kikusato et al. [15] have proposed a framework for the charge/discharge management of EV battery using the forecasted information of home and grid management system so that the PV array power is utilized maximally and very less power is drawn from the grid. Sun et al. [16] have proposed the strategy for minimizing the residential energy cost considering the driving pattern and the vehicle-to-grid (V2G) power transfer in EV integrated PV array and battery-based residential microgrid. Bhamidi et al. [17] have proposed the optimal planning and operational strategy of residential microgrid participating in demand side management. Yang et al. [18] have reported a strategy for distributed coordination of EV charging with renewable energy in the microgrid of building. Chaudhari et al. [19] have proposed a have developed a chance-constrained based control strategy for microgrid and the integrated EV. Turker et al. [21] have minimized the charging cost of the EV using vehicle to grid and vehicle to home functionality. Erdinc et al. [22] have proposed a smart household operation with bidirectional EV and energy storage. However, from the review, it is observed that the recent literature is dominated by the
control and single topological structure. Table I shows a comparison of the presented charger with the current literature. Therefore, in this paper, a household load integrated, grid connected solar PV array-based multifunctional EV charger is implemented with the combined control for achieving the satisfactory operation of various functionalities such as i) PV array MPPT without dc-dc converter, ii) four-quadrant operation of charger (V2G/G2V), iii) V2H with nonlinear load,
iv) active filtering, v) islanded/grid connected operation, vi) synchronization (automatic mode switching), vii) MPPT energy management in the overall system. Jafari et al. [26] have proposed a novel predictive fuzzy logic based energy management system for a grid-integrated microgrid, in which the controller utilizes the long term data of the system and predicts the energy generation, demand and the cost of the In the rule-based approach, the operation of the microgrid is decided by the heuristic rule. However, the drawback of the heuristic-based rule is that the rules are microgrid specific. Therefore, it is not possible to design the generalized rules. The centralized optimization [44] based energy management system uses the day-ahead forecast to optimize the microgrid operation. However, due to the high variability and uncertainty in the renewable generation, load and limited forecast accuracy, the day ahead scheduling cannot provide good performance. The droop control based power management scheme is also popular in microgrid [38], [45]. However, the selection of the droop gain for a wide range of operation is critical. To improve the gain tuning of the droop controller, low bandwidth communication is used. However, due to the low bandwidth of the communication channel, a delay introduces in the signal, which affects the gain tuning. Lin et al. [37] have proposed the distributed power management strategy for the multiple paralleled bi-directional interlinking converter. However, in this paper, a dc-link voltage regulation based energy management scheme is proposed, which uses only present dc-

voltage information for effective energy management. ver, it does not require any communication medium to
share the information. Therefore, this method is simple, cheap, reliable and easy to implement for the residential microgrid. Whereas the schemes presented in [46]-[47], require the past information, present information and information about other constraints affecting the system.

However, the effectiveness of the energy management scheme depends on the promptness and accuracy of the dc-link
for dc-link voltage regulation, so that both dynamic and steady- state performances of the system are improved. SMC is known for its excellent dynamic response and strong robustness to disturbances and uncertainties, such as unknown variations of control variables and system parameters [51]. The main contribution of this work involves assimilating various functionalities such as i) PV array MPPT without dc-dc converter, ii) four-quadrant operation of charger (V2G/G2V),
iii) V2H with nonlinear load, iv) active filtering, v) islanded/grid connected, vi) synchronization (automatic mode switching), vii) MPPT derating, viii) PCC voltage correction, in a single EV charger configuration, without the need of additional dc-dc converter for PV array, thereby reducing the cost of charger and improving the reliability of the charging and household supply. The advantage of this system is that a single system meets the requirements of household load, EV and the utility. The main features of this system are as follows.

- The use of PV array energy for EV charging and powering the household load, simultaneously in islanded and grid connected mode.
- Development of robust control strategy for generating a sinusoidal voltage at PCC, with total harmonic distortion (THD) less than 5%.
- The use of EV battery energy for supplying the household load uninterruptedly in islanded mode using vehicle-to-home (V2H) functionality.

TABLE I: STATE OF ART ON SOLAR PV ARRAY BASED EV CHARGER

S. No.	References	PV array without dc-dc Converter	Four Quadrant Operation (V2G/G2V)	V2H with nonlinear load	Active Filtering	Islanded / Grid Connected	Synchronization (Automatic Mode Switching)	MPPT Derating	PCC Voltage Correction
1	[23],[12],[27],[10],[11],[29],[38],[4]	No	No	No	No	Grid Connected	No	No	No
2	[24]	No	No	No	No	Both	Yes	No	No
3	[25],[26]	No	No	No	No	Both	No	No	No
4	[9]	No	No	No	Yes	Grid Connected	No	No	No
5	[28],[30],[31],[32],[33],[35]	No	Yes	No	No	Grid Connected	No	No	No
6	[34]	No	No	Yes	No	Both	No	No	No
7	[36],[37]	No	No	No	No	Islanded	No	No	No
8	[39]	No	No	No	No	Islanded	No	Yes	No
9	[40]	No	Yes	Yes	No	Both	Yes	No	No
10	Proposed system	Yes	Yes	Yes	Yes	Both	Yes	Yes	Yes

- Design of control for synchronizing the grid and PCC voltage and logic for generating the switch enabling logic (E) for a seamless transition between islanded to grid connected mode.
- Active power filter operation using VSC, so that the charger does not pollute the grid.
- On-demand vehicle-to-grid (V2G) reactive power capability using the VSC and the EV battery.
- In grid connected mode, voltage and current always comply with the IEEE-519 standard.
- Capability to operate under distorted voltage condition.
- A dc link voltage regulation based energy management strategy for all operating modes.
- A sliding mode control based robust dc-link voltage regulation, so that the energy management scheme performs its aforementioned tasks.

II. System Configuration

The circuit topology of the presented charging system is shown in Fig. 1. This system is a single-phase bi-directional charger for an EV that integrates the solar PV array directly on the dc-link of the VSC. This system charges the EV battery using the solar PV power/the grid power and feeds the solar PV / EV battery power into the grid. This charger is a two-stage charger, i.e. a bi-directional ac-dc conversion followed by the bi-directional dc-dc conversion stage. The ac-dc stage converts the input ac voltage into the dc voltage while charging the EV battery and works as an inverter to change the dc voltage into the ac voltage while feeding the solar PV power and EV power into the grid. The EV battery is connected to the output of the bi-directional dc-dc converter (BDDC). The dc-dc converter in this charger accomplishes the various tasks. While charging the EV battery, the dc converter works in buck mode and operates

Here *PPV*, *PEV*, *Ph* and *Pg* are solar PV array power, EV power, household load power and grid power, respectively. In this expression, the positive power represents the supplying of power, and negative power represents the consumption of power. This means that the EV and the grid can both supply and consume power. In grid connected mode, the charger undergoes the transient caused by the change in solar irradiance, household load and EV charging current. The change in the PV array power only affects the grid power and the charging/discharging of the EV battery and household supply should not be affected.

Therefore, a series of events occur to achieve the energy equilibrium in the system during irradiance change.

$$\text{Solar irradiance} \uparrow\downarrow \rightarrow P_{PV} \uparrow\downarrow \rightarrow \text{power at DC link} \uparrow\downarrow \rightarrow V_{dc} \uparrow\downarrow \rightarrow V_{dc}\ \text{regulation} \rightarrow I_P \uparrow\downarrow \rightarrow i^* \uparrow\downarrow \rightarrow_g i \uparrow\downarrow \quad (2)$$

Similarly, with the change in EV charging/discharging, the solar PV array power and the household supply remain unaffected, and the series of events for energy management during this transient, are as follows,

$$\text{charging power} \uparrow\downarrow \rightarrow I_{EV} \uparrow\downarrow \rightarrow \text{power at DC link} \downarrow\uparrow \quad (3)$$

$$\text{conversion} \rightarrow V_{dc} \downarrow\uparrow \rightarrow V_{dc}\ \text{regulation} \rightarrow I_P \uparrow\downarrow \rightarrow i^* \uparrow\downarrow \rightarrow_g i \uparrow\downarrow$$

In standalone mode, the energy management in the steady-state condition is given as,

$$P_{PV} \pm P_{EV} - P_h = 0 \quad (4)$$

in boost mode while discharging the EV battery.

Similar to the grid connected mode, the solar irradiance and household load change also disturb the energy equilibrium in standalone mode. However, the EV battery compensates for all disturbances in the power, as the dc-link voltage is controlled through the EV battery. Under the solar irradiance change, energy management is achieved as,

$$\text{Solar irradiance} \uparrow\downarrow \rightarrow P_{PV} \uparrow\downarrow \rightarrow \text{power at DC link} \uparrow\downarrow \rightarrow V_{dc} \uparrow\downarrow \rightarrow V_{dc} \text{ regulation} \rightarrow I^{*}_{EV} \uparrow\downarrow \rightarrow I_{EV} \uparrow\downarrow \quad (5)$$

Under household load change, energy management is achieved as,

$$i_h \uparrow\downarrow \rightarrow \text{power at DC link} P_{PV} \downarrow\uparrow \rightarrow V_{dc} \downarrow\uparrow \rightarrow V_{dc} \text{ regulation} \rightarrow I^{*}_{EV} \uparrow\downarrow \rightarrow I_{EV} \uparrow\downarrow \quad (6)$$

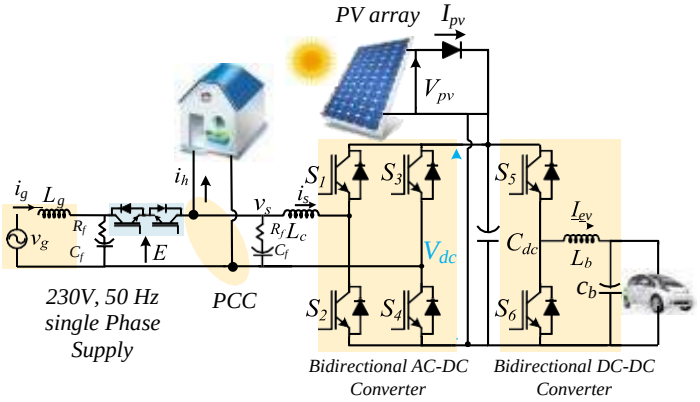

Fig. 1 Circuit topology of the charger

The maximum generated power from the solar PV array. The charger is connected to the grid through the coupling inductor (L_c). It is needed to eliminate the harmonics and to smoothen the grid current. A ripple filter is also connected at the PCC (Point of Common Coupling) to prevent the injection of switching harmonics generated by the VSC into the grid.

III. ENERGY MANAGEMENT STRATEGY

The energy management strategy of this charger is based on the regulation of constant dc-link voltage. The flow-chart of energy management under different operating conditions is shown in Fig. 2. The energy management in steady-state under grid connected mode is given as,

$$P_{PV} \pm P_B \pm P_g - P_h = 0 \quad (1)$$

IV. CONTROL ALGORITHM

The control objective is to charge the EV and supply the household load uninterruptedly irrespective of any disturbance. Therefore, the control is designed such that the multifunctional operation is achieved. The control is mainly divided into islanded and grid connected mode (GCM) as shown in Fig. 3 However, the vehicle-to-grid (V2G) active and reactive powers, vehicle-to-home (V2H) modes are covered in these two main controls. Moreover, the combined bi-directional dc-dc converter control for both islanded and grid connected modes are also discussed.

A. Grid Connected Mode Control

The purpose of GCM mode is to regulate the dc link voltage and the control the grid current for controlling the active and reactive power flow, thereby generating the switching pulses for the VSC. The sliding mode control (SMC) and VSC control are explained as follows.

1) Sliding Mode Control of dc Link Voltage

In this work, SMC is utilized for regulating the dc-link voltage and maximum power point tracking (MPPT) of the solar PV array. The dc-link voltage regulation is also required for the MPPT of the solar PV array, as in single-stage topology the

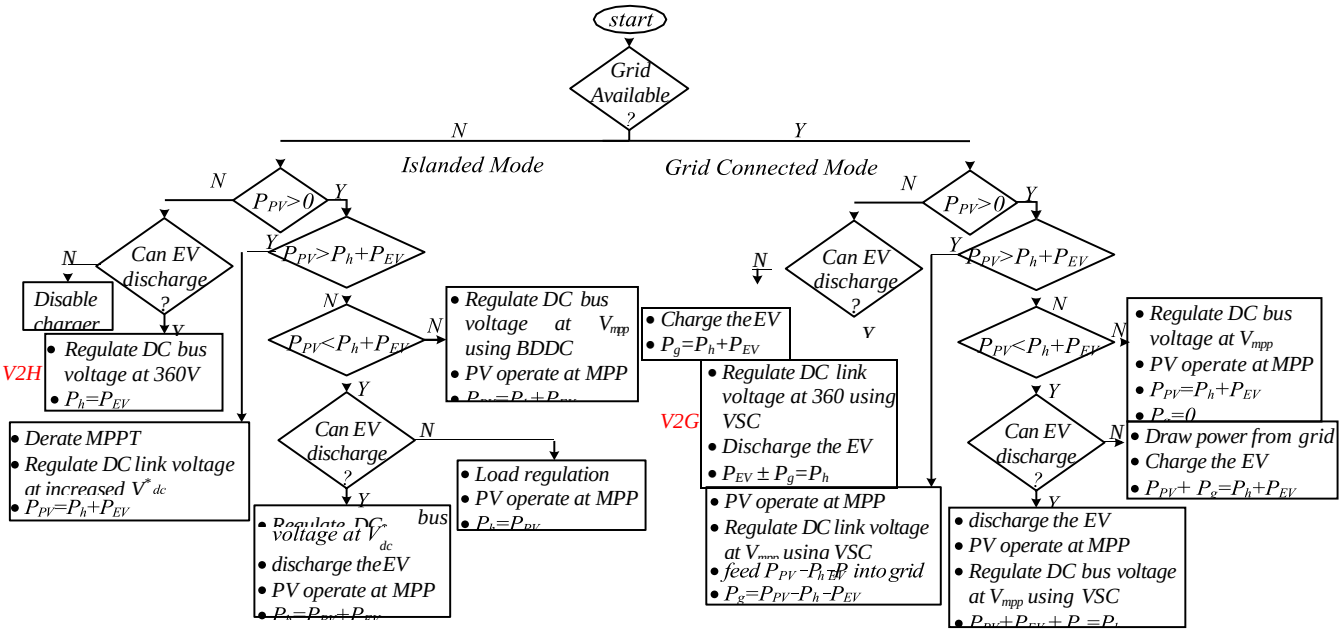

MPPT is achieved by regulating the dc-link voltage at the voltage of the solar PV array. The MPPT algorithm estimates the reference dc-link voltage (V_{dc}^*) at which the peak power of the solar PV array is extracted. However, in the absence of the solar PV generation, the dc-link voltage is regulated at a specific voltage (360V).

chattering cannot be fully eliminated with the used SMC

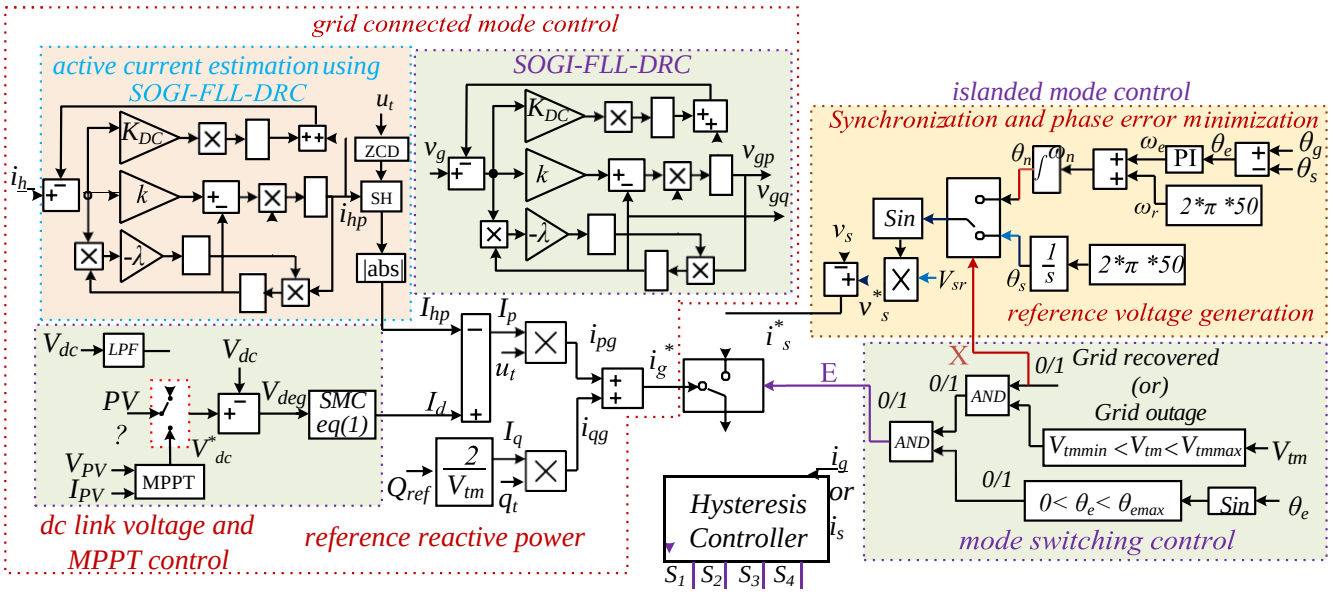

Due to the presence of (σ+δ)sign(S) in (16), the chattering phenomenon may appear with the used SMC control. The control. However, the chattering has been restricted to a certain frequency by defining the lowest allowable steady-state error by defining the value of δ such that the (σ+δ) does not become very small. Since σ is a positive constant, the δ is defined as,

$$\delta = \begin{cases} \| \quad \| & 0.1V \\ .1 & v_e < 0.1V \end{cases} \qquad (17)$$

2) VSC Control in GCM

VSC control is shown in Fig. 3. Due to the non-linear household loads and the EV, the grid current contains harmonics. Moreover, the power factor (PF) also deteriorates. Therefore, for improving the PF and ensuring the grid current THD within 5%, a second-order generalized integrator-frequency locked loop with dc rejection capability (SOGI-FLL-DR) [54] is used to estimate the fundamental load current so that the reference current becomes free of harmonics. Fig. 3 shows the extraction of fundamental active load current Using reference active grid current (ip) and component through sample hold with ZCD (Zero Crossing Detector). The expression for the active current estimation is given as [54],

$$\frac{i_{hp}}{i_h} = \frac{k\omega s^2}{s^3 + (k_o + k\omega)s^2 + \omega^2(s + k_o)} \qquad (18)$$

Where ih and ihp are loads and fundamental load currents. ω is frequency, k is a gain, which decides the speed of estimation, ko is the dc rejection coefficient, and λ is frequency estimation coefficient.

Using (16) and Ihp, the total active current is estimated as,

$$I_p = I_d - I_{hp} \qquad (19)$$

The amplitude of the reactive current (Iq) of the reference grid current (i'), is obtained on the basis of reference reactive power command ($Qref$) and it is given as,

$$I_q = \frac{2 \times Q_{ref}}{V_{tm}} \qquad (20)$$

Where V_{tm} is the amplitude of the PCC voltage (v_s).

The real (Ip) and reactive (Iq) components are multiplied with the in-phase (ut) and the quadrature-phase unit template (qt) to

obtain instantaneous reference active grid current (i_p) and instantaneous reference reactive grid current (i_q), and it is given as,

$$i_p = I_p \times u_t,\ i_q = I_q \times q_t \quad (21)$$

The in-phase (u_t) and the quadrature-phase unit template (q_t) are obtained using the following expressions,

$$u_t = \frac{v_{gp}}{V_{tm}},\ q_t = \frac{v_{gq}}{V_{tm}} \quad (22)$$

Where v_{gp} and v_{gq} are the in-phase and quadrature-phase voltage of PCC voltage (v_g) and V_{tm} is the amplitude of the PCC voltage. These two (vg and vs) voltages obtained using the SOGI-FLL- DR algorithm become free of harmonics, so that the estimated unit templates also become sinusoidal. Using vpg and vgq, the Vtm is obtained as,

$$V_{tm} = \sqrt{v_{gp}^2 + v_{gq}^2} \quad (23)$$

reference reactive
grid current (iq), the total reference grid current is obtained as,

$$i_g^* = i_p + i_q \quad (24)$$

This reference grid current (i_g^*) is compared with the sensed grid current (i_g) and the hysteresis controller generates the triggering signals for the VSC.

B. VSC Control in Islanded Mode

In islanded mode, the objective of the integrated system is to charge the EV and supply the household load autonomously using the PV array energy. Moreover, the V2H power transfer is utilized to feed the household load in the absence of the PV array energy. In islanded mode, the VSC is controlled to operate as an inverter to supply the load as per the control shown in Fig.3 For this, the controller generates the voltage using the reference frequency and reference voltage as shown in Fig. 3 Using the sensed voltage and the reference voltage, the pulses for the VSC are generated. While operating in the islanded mode, the charger needs to be connected to the grid for two-way power exchange. Therefore, it is required to match the PCC voltage, frequency and phase, to the grid voltage, frequency and phase. So that the connection to the grid becomes seamless and
automatic. Therefore, the controller estimates the phase angles of the PCC voltage and grid voltage and calculates the phase error between two voltages. The PI controller is used to minimize the phase error between two voltages. The PI controller translates the phase error information into error frequency. Using the error frequency, the controller generates the reference voltage of corrected frequency. As soon as, the phase of two voltages matches to each other, the controller generates the enabling signal for the bidirectional switch as per the switching logic shown in Fig. 3.

C. Bi-directional dc-dc Converter Control

The combined control of the bi-directional dc-dc converter for islanded and grid connected is exhibited in Fig. 4. In GCM, the EV battery is charged in constant current/constant voltage (CC/CV) mode and the cascade PI controller loop is used to control the charging of the EV battery. The outer PI controller controls the terminal voltage of the EV battery and gives the reference battery current for the current control. The reference current using a PI controller is given as,

$$I^{*}_{ev}(r) = I^{*}_{ev}(r-1) + k_{pv}\{V_{eve}(r) - V_{eve}(r-1)\} + k_{iv}V_{eve}(r) \quad (25)$$

Where V_{eve} is the dc-link voltage error and k_{pv}, k_{iv} are the gains of the PI controller.

For V2G power transfer, the reference current for discharging the EV battery is given by the user. The point to note here is that the sign of reference EV current for V2G mode is opposite of the G2V mode. Now using the reference EV current and the sensed EV currents, the error in the EV current is calculated and the inner PI control gives the duty cycle of the bi-directional dc- dc converter. The duty cycle is calculated as,

$$d_e(r) = d^{*}_{e}(r-1) + k_{pi}\{I_{eve}(r) - I_{eve}(r-1)\} + k_{ii}V_{eve}(r) \quad (26)$$

Where I_{eve} is the current error and k_{pi}, k_{ii} are the gains of the controller.

In islanded mode, the bi-directional dc-dc converter is used to regulate the dc-link voltage. Moreover, the MPP of the solar PV array is also achieved by regulating the dc-link voltage. For this, the MPPT algorithm gives the reference voltage of the dc-link for the MPP operation. However, in the absence of the PV array (V2H), the dc-link voltage is regulated at a specified voltage (V^{*} =360V) as shown in Fig. 4. In this condition also, cascaded PI control is used whose outer loop regulates the dc-link voltage and the inner loop controls the EV charging/discharging current. The expression of the outer loop is given as,

$$I^{*}_{ev}(r) = I^{*}_{ev}(r-1) + k_{pd}\{V_{de}(r) - V_{de}(r-1)\} + k_{id}V_{de}(r) \quad (27)$$

Where V_{de} is the voltage error. However, the gains of the controller are k_{pd} and k_{id}.

Now, (26) gives the duty cycle using reference and the sensed current. After this, the PWM generator gives switching signals for the converter.

V. RESULTS AND DISCUSSION

The EV charger designed for single-phase 230V, 50Hz grid is shown in Fig. 5. The open-circuit voltage and short circuit current of the solar PV array is 460V and 10A, respectively. However, the maximum power point voltage and current are 396 V and 9.5A, respectively. The lead-acid battery of 240V, 35Ah is used as an EV battery in the experimental prototype. The implementation of the charger is carried out using the digital controller (dSPACE-1006). For the implementation of the control algorithm, the digital controller requires various (voltage and current) signals of the charger. Therefore, various voltage and current signals (analog) are acquired using the Hall Effect based voltage (LEM LV-25P) and current (LEM LA-55P) sensor. These signals are converted into digital signals using an analog to digital converter (ADC). The digital controller uses the digital signal to implement the control algorithm and to generate the switching pulses for VSC and dc- dc converter.

The performance of the charger is shown in Figs. 6-13. The performance of the charger is evaluated in both steady-state and dynamic conditions. The steady-state performance of the charger is presented for the case when the solar PV array energy is used to charge the EV, feeds the local household load and supports the grid with surplus power. The dynamic performance of the charger is presented for various operating modes in both islanded and grid connected conditions. During implementation, the solar PV array power (PPV), the power drawn from the grid (P_g), and the power drawn from the EV (P_{EV}), are considered positive. However, the power fed into the grid, power drawn by the load and power drawn for EV charging is considered negative.

A. Steady-State Performance of Charger

Fig. 6 shows the experimental results in a steady-state condition. The steady-state behaviour of the charger is presented for the GCM, when the solar PV array power (P_{pv}) is used for EV charging, powering the local load and supporting the grid with the surplus power.

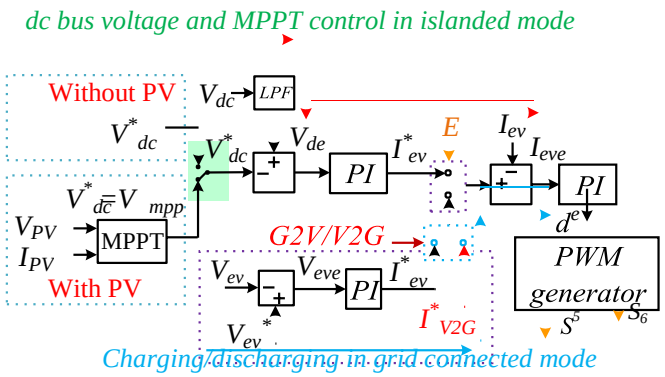

Fig. 4 Combined control strategy for bi-directional dc-dc converter

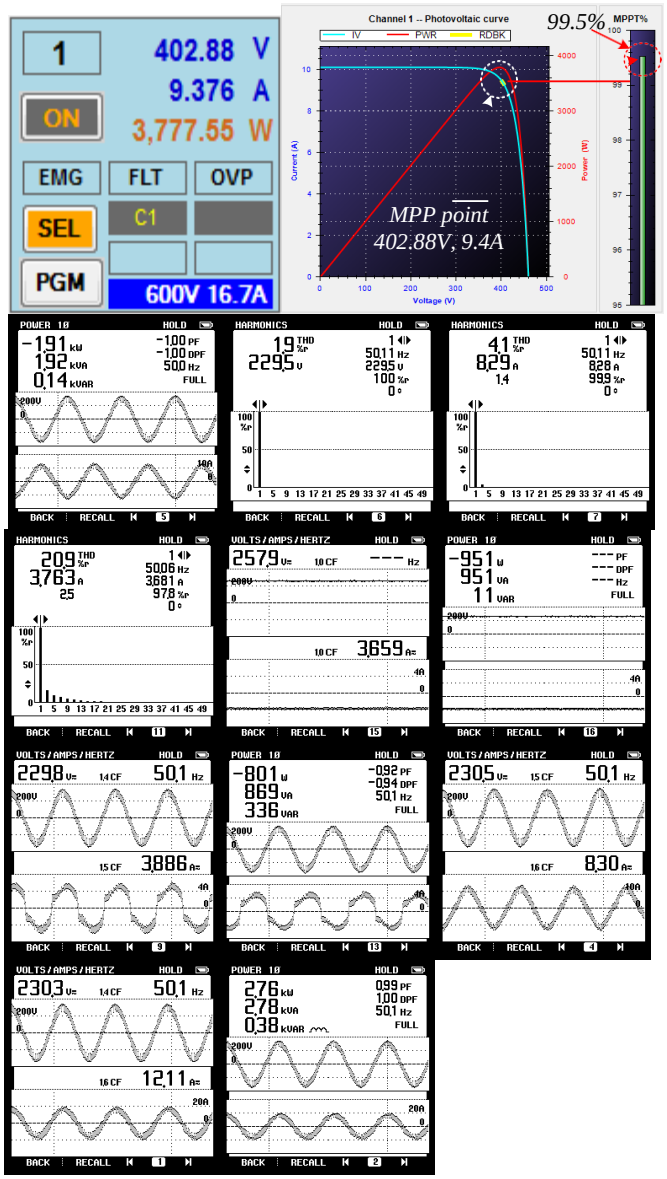

Fig. 6 Steady state performance in grid connected mode, (a)-(b) *VPV*, *IPV* and *PPV*, (c)-(d) *vh*,*ih* and *Ph*, (e)-(f) *vg*, *ig* and *Pg*, (g)-(i) harmonic spectrum of *vg*, *ig* and *ih*, (j)-(k) *Vev*,*Iev* and *Pev*, (l)-(m) *vc*, *ic* and *Pc*

Figs. 6 (a)-(b) show that the solar PV array is generating 3.77kW. Out of 3.77 kW, 0.8kW is taken by the household load (Ph) and 0.95kW is used by the EV for charging. Remaining 1.91kW is fed into the grid at UPF. The voltage (VPV), current (IPV) and power (PPV) of the solar PV array are shown in Figs. 6(a)-(b). The voltages, currents and powers of the load and the EV battery are shown in Figs. 6 (c)-(d) and Figs. 6 (j)-(k). The voltage (vg), current (ig), and power of the grid (Pg) are shown in Figs. 6 (e)-(f). The charger is not injecting any voltage and current harmonics into the grid as shown by the grid voltage (vg), grid current (ig) and load current (ih), total harmonic distortion (THD) in Figs. 6 (g)-(i). Moreover, it is also not drawing any reactive power from the grid as justified by the unity displacement power factor (DPF) operation of the charger in Fig. 6 (f). Fig. 6 (l)-(m) show the VSC parameters.

B. Dynamic Performance of Charger

The islanded mode of the charger is presented to show the charger capability to operate autonomously using the solar PV array energy for providing the charging facility to the EV and supply to the household load. During the islanded mode of operation, the household load changes along with the solar irradiance. Therefore, the charger performance under these disturbances is presented in Fig. 7. Initially, the solar PV array charges the EV and feed the household load as shown by the negative EV current in Fig. 7(a). However, after some time, the solar PV array generation (P_{pv}) becomes zero. Therefore, to feed the load uninterruptedly, the EV battery starts discharging, to support the home loads, as shown by the positive battery current (Iev) in Fig. 7 (a). This mode is called vehicle to home. Fig. 7 (b) shows the voltage generated at the PCC (v_S) using the charger. Moreover, the non-sinusoidal load current (ih) is also exhibited in Fig. 7 (b). Fig. 7(b) exhibits that during solar irradiance change the PCC voltage (v_S), load current (ih) and dc-link voltage (V_{dc}) are undisturbed.

The islanded operation under load change is shown in Figs. 7(c)-(d). Here, the load is changed in step over a wide range. The dc-link voltage is maintained by the bi-directional dc-dc converter, the load change is compensated by the EV battery. Because of which, the EV battery charging changes with the load change. However, the solar PV array generation (Ppv) and the dc-link voltage (V_{dc}) are not affected by the load change. Fig. 7(d) also shows that the connection/disconnection of the household load is not disturbing the PCC voltage. Fig. 7 (d) shows that when the load is disconnected, the whole solar PV array power (Ppv) is stored into the EV battery. However, the MPP operation of the solar PV array is not affected.

In Figs. 7 (e)-(f), the solar irradiance is changed in steps, keeping the household constant. Initially, with the increase in solar irradiance, PV power increases. As a result, the power stored in the EV battery also increases to maintain the active power balance. However, when the solar irradiance is increased from 500W/m^2 to 1000W/m^2, the solar PV array generation does not increase because the controller increases the reference dc-link voltage to achieve the MPPT derating as the charging rate of EV is restricted by the controller as shown in Fig. 7.

The charger operates in grid connected mode either due to the excess power generation or power scarcity. In both cases, the charger exchanges the power with the grid at unity power factor. However, in grid connected mode also, many disturbances occur during the operation. Therefore, the stable operation of the charger under these operating condition is required. The behaviour under the load perturbation in GCM is shown in Fig.
8. In grid connected mode, the dc-link voltage is regulated by the voltage source converter of the charger, therefore, the load change only affects the grid power. Here, the load is changed in steps and the corresponding change in grid power (Pg) can be seen in Fig. 8(a). The reduction in load current (ih) is causing an increase in grid current (ig) as shown in Fig. 8(b). However, the PV array current (I_{pv}) and the EV charging current (Iev) are not affected by the load change. The same is justified by the undisturbed PV array (P_{pv}) and the EV power (P_{ev}). The voltage across the dc link (V_{dc}) is also regulated during the load change. The performance under solar irradiance change is shown in Figs. 8(c)-(d). Due to the change in the solar irradiance level, the PV array generation (P_{pv}) changes. Since the household loads and the EV charging should not be disturbed by the irradiance change, the grid power (Pg) changes to maintain the power balance. The solar irradiance is changed in step from 1000W/m^2 to 700W/m^2, 700W/m^2 to 300W/m^2 and so on. Due to this, the grid power (Pg) becomes both positive and negative. That means, at 1000W/m^2, the excess generation is supplied back to the grid. However, at 300W/m^2, the power is drawn from the grid. The EV power (Pev), load power (Ph) anddc-link voltage (V_{dc}) remain undisturbed.

In GCM, the EV charger participates in demand based active power exchange with the grid. Therefore, the EV voluntarily takes active power from the grid or discharges some of its stored energy to the grid as shown in Figs. 8 (e)-(f). Due to the charging /discharging of the EV battery, the grid power (Pg) changes without affecting the PV array generation (Ppv) and the load supply (Ph). Figs. 8(e)-(f) show the step change in the battery current (Iev) from charging to discharging. Due to the discharging of the battery, the grid current (ig) increases. However, the PV array current (Ipv) and the dc-link voltage (Vdc) remain unaltered. Therefore, from the dynamic results, it is observed that the charger operation in grid connected and islanded mode are not affected by the disturbances. Moreover, it is also perceived that one type of perturbation is not interfering with the operation of another component.

Fig. 9 shows the V2G reactive power performance at Pg=0kW. Due to the step-change in the reference reactive power ($Qref$) from 1kVAR to -1kVAR, the grid current (ig) becomes leading from lagging. Moreover, the dc-link voltage

(*Vdc*) remains undisturbed.

Fig. 10 shows the harmonic compensation and PCC voltage correction capability of the charger. Fig. 10 shows that the grid current (*ig*) is the same as load current (*ih*) without harmonics mitigation using VSC. However, it is observed that the grid current (*ig*) becomes sinusoidal after harmonics compensation. The current (*is*) of VSC is

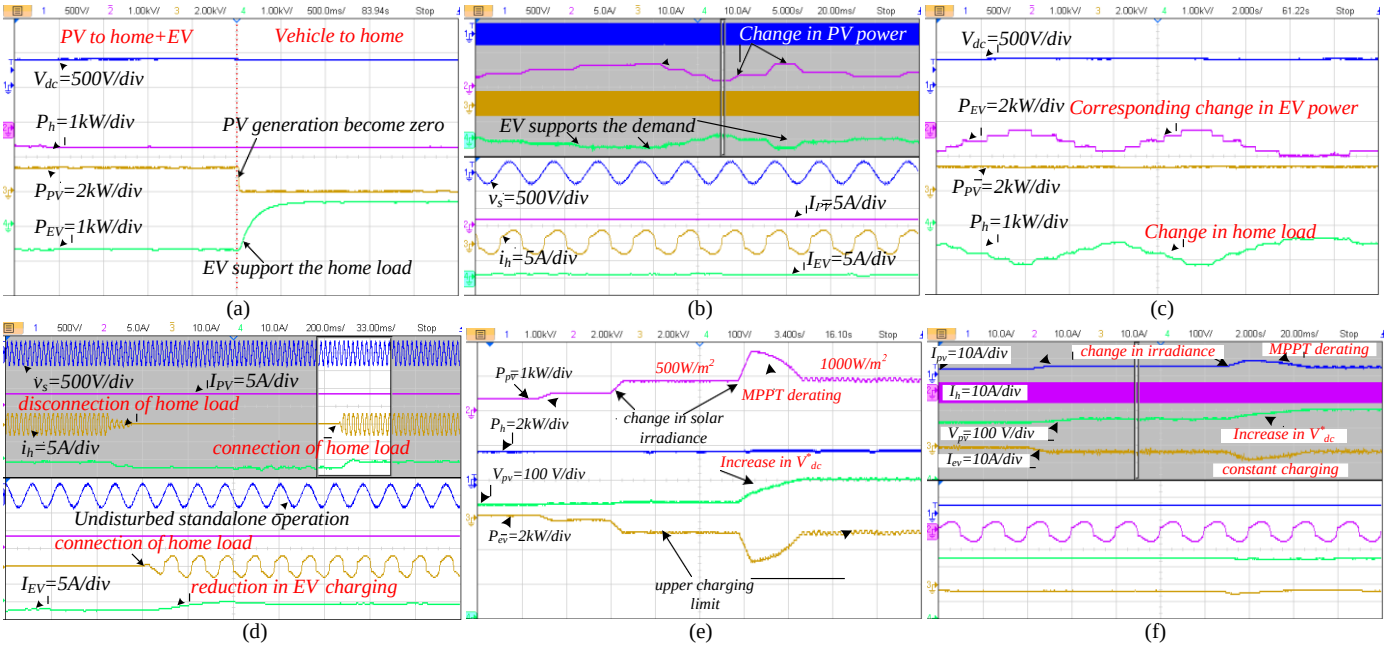

Fig. 7 Dynamic performance in islanded condition, (a)-(b) under solar irradiance change, (c)-(d) under the change in household load, (e)-(f) derating of MPPT

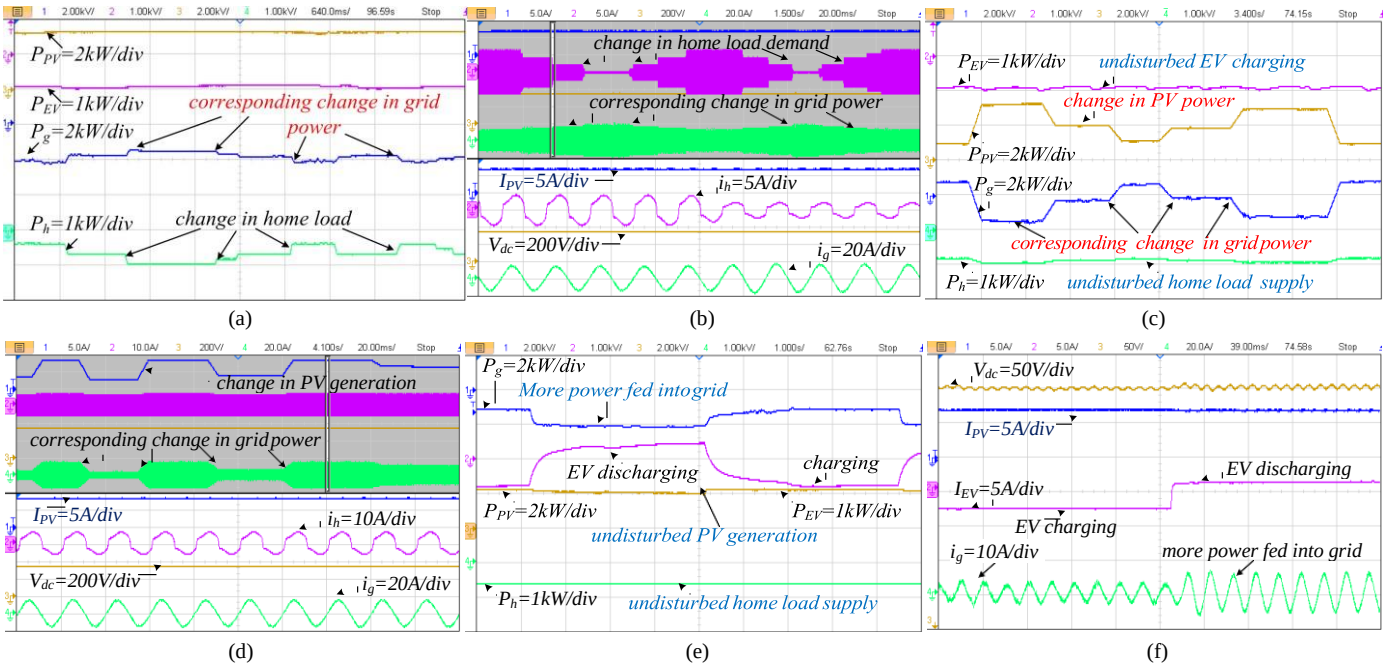

Fig. 8 Dynamic performance in grid connected mode, (a)-(b) under change in household load, (c)-(d) under change in solar irradiance power, (e)-(f) under change in charging/discharging of EV battery

leading from lagging. Moreover, the dc-link voltage (*Vdc*) remains undisturbed.

Fig. 10 shows the harmonic compensation and PCC voltage correction capability of the charger. Fig. 10 shows that the grid current (*ig*) is the same as load current (*ih*) without harmonics mitigation using VSC.

.

However, it is observed that the grid current (*ig*) becomes sinusoidal after harmonics compensation. The current (*is*) of VSC is shown in Fig. 10. Moreover, it is observed that the PCC voltage (*vg*) profile also improves due to compensation

C. Comparison of dc Link Voltage Regulation Using PI Control and SMC Control

Fig. 12 shows the dc-link voltage (Vdc) regulation capability of the PI controller and SMC under the step change of 50V in reference dc-link voltage (V^*). From Fig. 12, it is observed that the SMC is faster in regulating the dc-link voltage as compared the PI control.

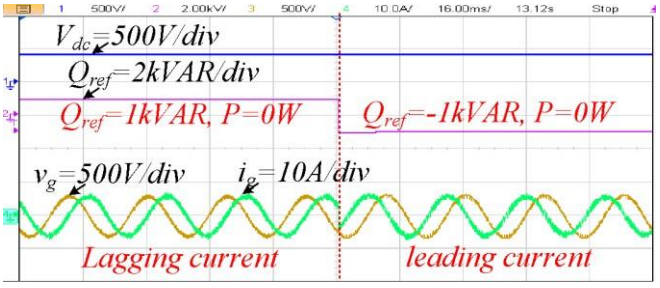

Fig. 9 Performance of vehicle to grid reactive power support

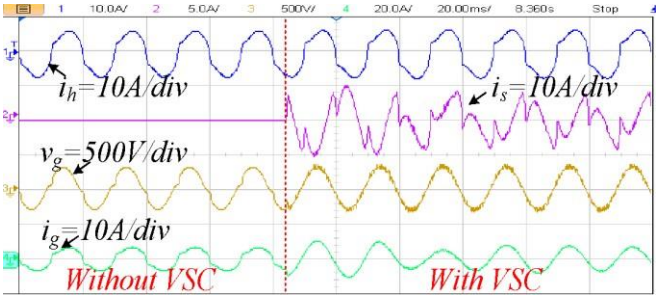

Fig. 10 Performance under distorted voltage condition and active power filter operation

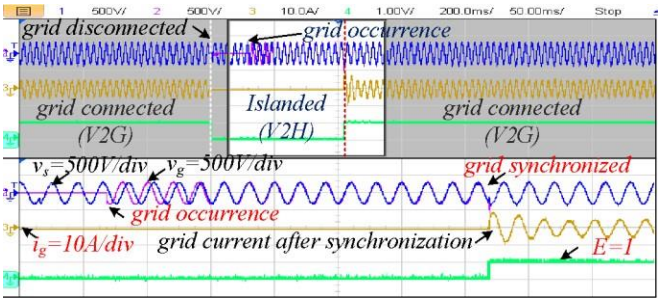

Fig. 11 Synchronization, mode switching and enabling signal generation

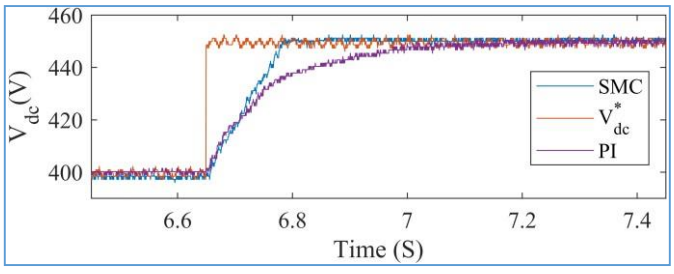

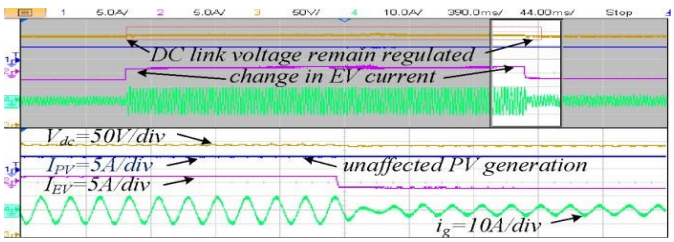

Performance Comparison of SMC and PI Control at Sudden Change in Charging/Discharging Current of EV

Due to sudden variation in EV current (Iev) from discharging to charging, the dc-link voltage (Vdc) is not regulated with the PI control, as shown in Fig. 13 (a). However, the SMC control has regulated the dc-link voltage (Vdc) at the sudden change, as shown in Fig. 13 (b). Since the PV array MPP operation depends on the dc-link voltage regulation at MPP voltage; the PV array does not operate at MPP due to the steady-state error in PI control. Moreover, it also changes under the sudden change in EV current. However, with SMC, the steady-state error is always zero and it also does not change with EV current change. Therefore, it always operates at MPP.

VI. CONCLUSION

An integrated charger with solar PV array, household load and grid has been implemented using the IGBT switches based converters, solar simulator, EV battery, dSPACE (1006) controller and the test results have verified the simultaneous EV charging and household supply in both islanded and grid connected modes. From these test results, it is observed that this charger is performing its specified task of EV charging, supplying local loads and maintaining the power quality at the grid side. Moreover, the islanded operation with voltage THD less than 5% and vehicle to home operation using solar PV array is also verified. The demand-based reactive power support and the active power filtering using VSC are also validated through test results. The smooth transition from islanded to grid connected mode and vice versa are verified by test results.

REFERENCES

[1] J. R. Aguero, E. Takayesu, D. Novosel and R. Masiello, "Modernizing the Grid: Challenges and Opportunities for a Sustainable Future," *IEEE Power and Energy Magazine*, vol. 15, no. 3, pp. 74-83, May-June 2017.

[2] D. Bowermaster, M. Alexander and M. Duvall, "The Need for Charging: Evaluating utility infrastructures for electric vehicles while providing customer support," *IEEE Electrifi. Mag.*, vol. 5, no. 1, pp. 59-67, 2017

[3] X. Lu and J. Wang, "A Game Changer: Electrifying Remote Communities by Using Isolated Microgrids," *IEEE Electrifi. Mag.*, vol. 5, no. 2, pp. 56- 63, June 2017.

[4] T. Ma and O. A. Mohammed, "Optimal Charging of Plug-in Electric Vehicles for a Car-Park Infrastructure," *IEEE Trans. Ind. Applicat.*, vol. 50, no. 4, pp. 2323-2330, July-Aug. 2014.

[5] L. Cheng, Y. Chang and R. Huang, "Mitigating Voltage Problem in Distribution System With Distributed Solar Generation Using Electric Vehicles," *IEEE Trans. Sust. Ene*, vol. 6, no. 4, pp. 1475-1484, Oct. 2015.

[6] S. J. Gunter, K. K. Afridi and D. J. Perreault, "Optimal Design of Grid- Connected PEV Charging Systems With Integrated Distributed Resources," *IEEE Trans. Smart Grid*, vol. 4, no. 2, pp. 956-967, 2013.

[7] O. Erdinc, N. G. Paterakis, T. D. P. Mendes, A. G. Bakirtzis and J. P. S. Catalão, "Smart Household Operation Considering Bi-Directional EV and ESS Utilization by Real-Time Pricing-Based DR," *IEEE Trans. Smart Grid*, vol. 6, no. 3, pp. 1281-1291, May 2015.

[8] H. R. Baghaee, M. Mirsalim, G. B. Gharehpetian and H. A. Talebi, "A Decentralized Power Management

[9] Z. Yi, W. Dong and A. H. Etemadi, "A Unified Control and Power Management Scheme for PV-Battery-Based Hybrid Microgrids for Both Grid-Connected and Islanded Modes," *IEEE Trans. Smart Grid*, vol. 9, no. 6, pp. 5975-5985, Nov. 2018.

[10] M. Kwon and S. Choi, "Control Scheme for Autonomous and Smooth Mode Switching of Bidirectional DC–DC Converters in a DC Microgrid," *IEEE Trans. Power Electronics*, vol. 33, no. 8, pp. 7094-7104, Aug. 2018.

[11] M. Jafari, Z. Malekjamshidi, J. Zhu and M. Khooban, "Novel Predictive Fuzzy Logic-Based Energy Management System for Grid-connected and Off-grid Operation of Residential Smart Micro-grids," *IEEE Journal of Emerging and Selected Topics in Power Electronics*, Early Access.

[12] S. A. Singh, G. Carli, N. A. Azeez and S. S. Williamson, "Modeling, Design, Control, and Implementation of a Modified Z-Source Integrated PV/Grid/EV DC Charger/Inverter," *IEEE Trans. Industrial Electronics*, vol. 65, no. 6, pp. 5213-5220, June 2018.

[13] M. Restrepo, J. Morris, M. Kazerani and C. A. Cañizares, "Modeling and Testing of a Bidirectional Smart Charger for Distribution System EV Integration," *IEEE Trans. Smart Grid*, vol. 9, no. 1, pp. 152-162, 2018.

[14] J. Y. Yong, V. K. Ramachandaramurthy, K. M. Tan and J. Selvaraj, "Experimental Validation of a Three-Phase Off-Board Electric Vehicle Charger With New Power Grid Voltage Control," *IEEE Trans. Smart Grid*, vol. 9, no. 4, pp. 2703-2713, July 2018.

[15] M. Nikkhah Mojdehi and P. Ghosh, "An On-Demand Compensation Function for an EV as a Reactive Power Service Provider," *IEEE Trans. Vehicular Technology*, vol. 65, no. 6, pp. 4572-4583, June 2016.

[16] U. R. Prasanna, A. K. Singh and K. Rajashekara, "Novel Bidirectional Single-phase Single-Stage Isolated AC–DC Converter With PFC for Charging of Electric Vehicles," *IEEE Trans. Transportation Electrification*, vol. 3, no. 3, pp. 536-544, Sept. 2017.

[17] D. B. Wickramasinghe Abeywardana, P. Acuna, B. Hredzak, R. P. Aguilera and V. G. Agelidis, "Single-Phase Boost Inverter-Based Electric Vehicle Charger With Integrated Vehicle to Grid Reactive Power Compensation," *IEEE Trans. Power Electron.*, vol. 33, no. 4, pp. 3462- 3471, April 2018.

[18] N. Mehboob, M. Restrepo, C. A. Cañizares, C. Rosenberg and M. Kazerani, "Smart Operation of Electric Vehicles With Four-Quadrant Chargers Considering Uncertainties," *IEEE Trans. Smart Grid*, vol. 10, no. 3, pp. 2999-3009, May 2019.

[19] F. Berthold, A. Ravey, B. Blunier, D. Bouquain, S. Williamson and A. Miraoui, "Design and Development of a Smart Control Strategy for Plug- In Hybrid Vehicles Including Vehicle-to-Home Functionality," *IEEE Trans. Transportat. Electrification*, vol. 1, no. 2, pp. 168-177, Aug. 2015.

[20] H. N. de Melo, J. P. F. Trovão, P. G. Pereirinha, H. M. Jorge and C. H. Antunes, "A Controllable Bidirectional Battery Charger for Electric Vehicles with Vehicle-to-Grid Capability," *IEEE Trans. Vehicular Technology*, vol. 67, no. 1, pp. 114-123, Jan. 2018.

[21] H. Mahmood and J. Jiang, "Autonomous Coordination of Multiple PV/Battery Hybrid Units in Islanded Microgrids," *IEEE Trans. Smart Grid*, vol. 9, no. 6, pp. 6359-6368, Nov. 2018.

[22] P. Lin, P. Wang, C. Jin, J. Xiao, X. Li, F. Guo, and C. Zhang., "A Distributed Power Management Strategy for Multi-Paralleled Bidirectional Interlinking Converters in

Hybrid AC/DC Microgrids," *IEEE Trans. Smart Grid*, vol. 10, no. 5, pp. 5696-5711, Sept. 2019.

[23] M. O. Badawy and Y. Sozer, "Power Flow Management of a Grid Tied PV-Battery System for Electric Vehicles Charging," *IEEE Trans. Industry Applications*, vol. 53, no. 2, pp. 1347-1357, March-April 2017.

[24] Q. Yang, L. Jiang, H. Zhao and H. Zeng, "Autonomous Voltage Regulation and Current Sharing in Islanded Multi-Inverter DC Microgrid," *IEEE Trans. Smart Grid*, vol. 9, no. 6, pp. 6429-6437, 2018.

[25] V. Monteiro, J. G. Pinto and J. L. Afonso, "Operation Modes for the Electric Vehicle in Smart Grids and Smart Homes: Present and Proposed Modes," *IEEE Trans. Veh. Techno.*, vol. 65, no. 3, pp. 1007-1020, 2016.

[26] S. Boudoudouh and M. Maaroufi, "Renewable Energy Sources Integration and Control in Railway Microgrid," *IEEE Trans. Ind. Appl.*, vol. 55, no. 2, pp. 2045-2052, March-April 2019.

[27] C. Luo, Y. Huang and V. Gupta, "Stochastic Dynamic Pricing for EV Charging Stations With Renewable Integration and Energy Storage," *IEEE Trans. Smart*, "Operational Value Based Energy Storage Management for Photo-Voltaic(PV) Integrated Active Power Distribution Systems," *IEEE Trans. Ind. Appl.*, Early Access.

AUTHORS

L Suresh was born in Tiruchanoor (AP), India, in 1987. He received B. Tech. degree in Electrical and Electronics Engineering from Siddharth Institute of Engineering and Technology ,Puttur (AP), India, in 2009 and M. Tech. degree in Power Electronics & Electrical Drives from SVPCET, Puttur in 2013. He is currently working as a Assistant Professor in Department of Electrical Engineering, VEMU Institute of Technology,P.Kothakota, Chittoor. His areas of interests include electric vehicle, renewable energy based charging infrastructure, power electronics, renewable energy, micro-grid, and power quality.He has more than 12 years of experience in teaching.

P Shameem currently persuing M.Tech(PE&ED) bearing roll no 184M1D5405 in Vemu Institute of Technology, P.Kothakota-Chittoor.Her areas of interest are Control Systems and Power Electronics.